# Rational molecular design for achieving persistent and efficient pure organic room-temperature phosphorescence

*Weijun Zhao[1,§], Zikai He[1,§], Jacky, W. Y. Lam[1], Huili Ma[2], Gongxun Bai[3], Jianhua Hao[3], Qian Peng[2,*] and Ben Zhong Tang[1,4,5,*]*

[1]Department of Chemistry, Division of Life Science, State Key Laboratory of Molecular Neuroscience, Institute for Advanced Study, Institute of Molecular Functional Materials, Division of Biomedical Engineering, Hong Kong Branch of Chinese National Engineering Research Center for Tissue Restoration and Reconstruction, The Hong Kong University of Science and Technology (HKUST), Clear Water Bay, Kowloon, Hong Kong, China

[2]Key Laboratory of Organic Solids, Beijing National Laboratory for Molecular Science (BNLMS), Institute of Chemistry, Chinese Academy of Sciences, Beijing 100190, China

[3]Department of Applied Physics, The Hong Kong Polytechnic University, Hong Kong, China

[4]HKUST Shenzhen Research Institute, No. 9 Yuexing First RD, South Area, Hi-tech Park Nanshan, Shenzhen 518057, China

[5]Guangdong Innovative Research Team, SCUT-HKUST Joint Research Laboratory, State Key Laboratory of Luminescent Materials and Devices, South China University of Technology (SCUT), Guangzhou 510640, China

[§]The authors contributed equally to this work.

[*]Correspondence and requests for materials should be addressed to B.Z.T. or Q.P. (tangbenz@ust.hk or qpeng@iccas.ac.cn)

## Abstract

**The manipulation of the emission properties of purely organic room temperature phosphors through molecular design has been attractive but challenging. Tremendous efforts have been put into modulating the aggregation behaviors to suppress nonradiative decay. However, the goal of generating the room temperature phosphorescence with high efficiency and long lifetime has been met with limited success. Here, we present a rational design principle for achieving the goal based on molecular structure engineering. Comprehensive investigations on molecular orbitals reveal that the exciton configuration is crucial to intersystem crossing and radiative phosphorescence decay. Tailoring the aromatic subunits in aryl phenones can effectively tune energy level and orbital feature of triplet exciton. Our experimental data reveals that a series of color-tunable pure organic phosphors with balanced lifetime and efficiency can be realized under ambient conditions, demonstrating the validity of our instructive design principle.**

Light, emitted from luminophores, is one of the most fundamental and indispensable elements to life and society. The development of luminophores has greatly promoted high-tech innovations in energy and life science. For instance, luminescent materials are widely used in organic light-emitting diodes and biotechnologies. Particularly, luminophores with phosphorescence can potentially utilize 75% electrically generated triplet excitons[1] and function as high-sensitivity bioimaging probes for elimination of short-lived autofluorescence[2]. Phosphorescence materials now find varied applications in electronics[3,4], optics[5,6] and biological area[7]. As emitting from the excited triplet state which is sensitive towards temperature and oxygen[8], phosphorescence is normally observed at cryogenic and inert conditions that severely restrict its applications. Achieving persistent and efficient room temperature phosphorescence (RTP) therefore draws extensive attentions. So far, most efficient RTP luminogens are limited to metal-containing inorganic and organometallic compounds that

usually suffer from high cost and cytotoxicity, difficult processing, low flexibility and stability[9,10]. As attractive alternatives, purely organic RTP materials enjoy the advantages of wide variety[11], good biocompatibility[12], appreciable stability and good processability[13,14]. However, developing persistent and efficient purely organic RTP materials is extremely difficult because of weak spin–orbit coupling and rapid nonradiative decay rate.

Recently, several groups have applied different methodologies including polymer aggregation[15], crystallization[16,17], halogen bonding[18,19], matrix assisting[20,21], self-assembly[22,23], and H-aggregation[24], etc to obtain the purely organic RTP systems (Figure 1). Tremendous effort have been put into modulating the aggregation behaviors to suppress nonradiative decay pathways of organic phosphors[25]. We classify these strategies as aggregation-induced RTP (Figure 1). Despite of these exciting ahievements[26], seldom examples with both high efficiency and long lifetime are obtained. It is also quite difficult to extend the strategies among the systems for lacking a comprehensive investigation on molecular structure-property relationship.

Here we develop a structure-property relationship and a derived molecular design principle based on the molecular orbital investigations. This work provides rational guidelines that will undoubtedly promote the fundamental understanding and exploration of novel purely organic RTP systems based on molecular structure. Novel phosphors with high efficiency and long lifetime as well as tunable emission are developed as a proof-of-concept. Especially, experimental data reveals that balanced RTP performance could be achieved upon one molecule.

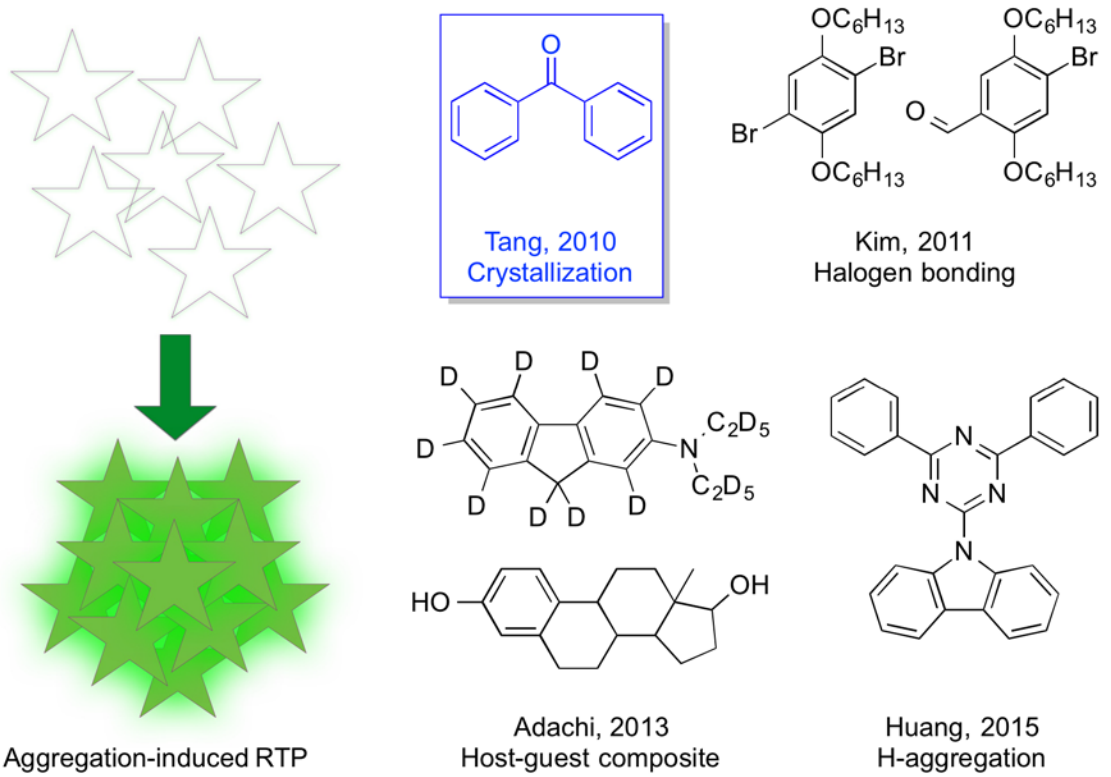


**Figure 1 | Strategies for achieving purely organic RTP system.** Schematic representation of modulating the aggregation behaviors of organic phosphors to suppress nonradiative decay pathways for RTP that are classified as the aggregation-induced RTP. Selected representatives of purely organic RPT materials applying different aggregation methodologies.

## Results and discussion

### Molecular Orbital Model

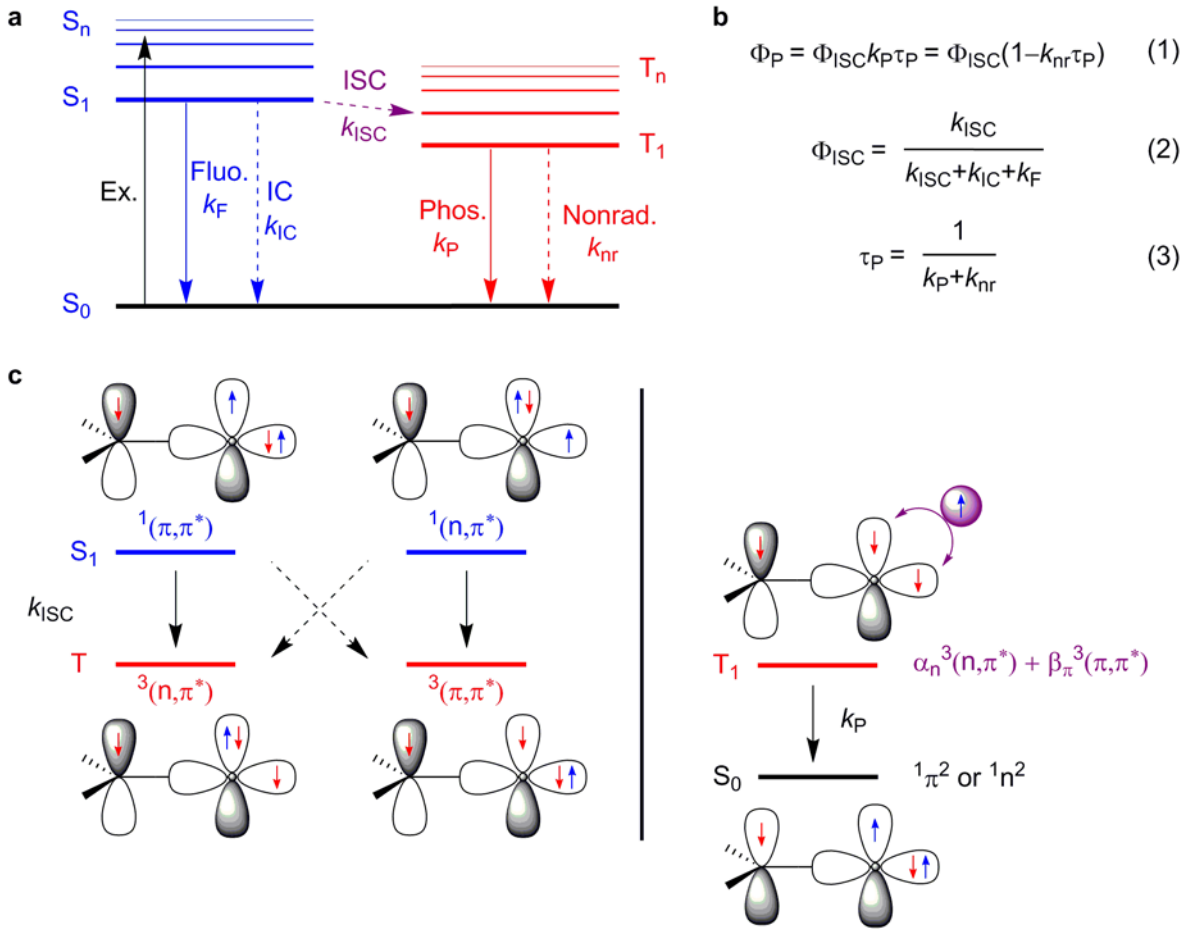


**Figure 2 | Theoretical models for understanding the performance of purely organic RTP. a**, A Jablonski diagram of organic luminogens is presented. **b**, Equations of phosphorescence quantum yield, intersystem quantum yield, and phosphorescence lifetime. **c**, Schematic representation of El-Sayed rule for intersystem crossing and molecular orbital hybridization of the lowest triplet states for tunable phosphorescence decay rate. Note that the typical persistent organic phosphorescence results from extremely slow radiative decay rate of $T_1$ with pure $^3(\pi,\pi^*)$ configuration.

The Jablonski diagram (Figure 2a) lists the typical decay pathways of the lowest singlet ($S_1$) and triplet ($T_1$) excited states. The efficient (high phosphorescence quantum yield $\Phi_P$) and persistent (long phosphorescence lifetime $\tau_P$) RTP materials require the high quantum yield of intersystem crossing ($\Phi_{ISC}$) and the slow relaxation process of $T_1$ in which the phosphorescence is the dominant decay pathway (Equation (1)).

High $\Phi_{ISC}$ is built upon the much larger intersystem crossing (ISC) rate $k_{ISC}$ to compete with fluorescence decay rate $k_F$ and internal conversion decay rate $k_{IC}$ in the depopulating processes of $S_1$ (Equation (2)). The $k_{ISC}$ can be greatly promoted by small singlet-triplet splitting energy, high mixing degree of the singlet and triplet molecular orbital configurations, and effective spin-orbital coupling (SOC). Some special moieties such as inorganic metals (for example, Ir and Pt), heavy halogen, heteroatom and deuterated carbons etc can trigger the effective SOC. For purely organic compounds without heavy halogen atoms, according to the El-Sayed rule (Figure 2c)[27], the effective SOC occurs when crossing either from $^1(\pi,\pi^*)$ to $^3(n,\pi^*)$ or from $^1(n,\pi^*)$ to $^3(\pi,\pi^*)$. The non-bonding (n) orbital make single-center $p_x \rightarrow p_y$ transition available to provide essential angular momentum during ISC process. Note that n orbital need to be perpendicular to $\pi$ orbital to facilitate such transition. In contrast, the intersystem crossing neither from $^1(\pi,\pi^*)$ to $^3(\pi,\pi^*)$ nor $^1(n,\pi^*)$ to $^3(n,\pi^*)$ is not flavored in which the SOC is ineffective for lacking readily single-center $p_x \rightarrow p_y$ transition to provide essential

momentum. Existence of n orbital becomes crucial to trigger effective SOC and promote the ISC process.

The persistent purely organic RTP materials ($\tau_P$ ~s) require the slow relaxation process of $T_1$. As a result, the phosphorescence decay rate $k_P$ should be even lower (Equation (3)). Normally, only the $T_1$ with the pure $^3(\pi,\pi^*)$ configuration can give such slow decay rate (~$10^0$ $s^{-1}$) as transition from $^3(\pi,\pi^*)$ to $^1\pi^2$ is forbidden in terms of electron-spin according to the El-Sayed rule[28]. If the $T_1$ is a pure $^3(n,\pi^*)$ configuration, it can give much faster decay rate (~$10^2$ $s^{-1}$) as transition from $^3(n,\pi^*)$ to $^1n^2$ is preferred. In purely organic compounds, the $T_1$ maybe neither pure $^3(\pi,\pi^*)$ nor pure $^3(n,\pi^*)$, but a hybrid mixture of the two configurations with different proportion: $\alpha_n{}^3(n,\pi^*)+\beta_\pi{}^3(\pi,\pi^*)$ ($\alpha_n+\beta_\pi = 1$, Figure 2c). The $T_1$ with the hybrid configuration will give the moderate and tunable $k_P$. An ideally persistent purely organic phosphor requires its $T_1$ having a nearly pure $^3(\pi,\pi^*)$ configuration ($\beta_\pi$ is close to 1).

Finally, the phosphorescence is the dominant decay pathway of $T_1$ requires that $k_P$ is much larger than $k_{nr}$. However, in purely organic compounds, the $k_P$ is normally too small to compete with $k_{nr}$. The widely used method to enhance the RTP efficiency is the suppression of $k_{nr}$. Theoretically, the $k_{nr}$ can be reduced by control of the nuclear configuration change during excited state relaxation. Experimentally, enhancement of the molecular rigidity (structural or environmental constraint) is a widely used and powerful tool to suppress the $k_{nr}$[12–25].

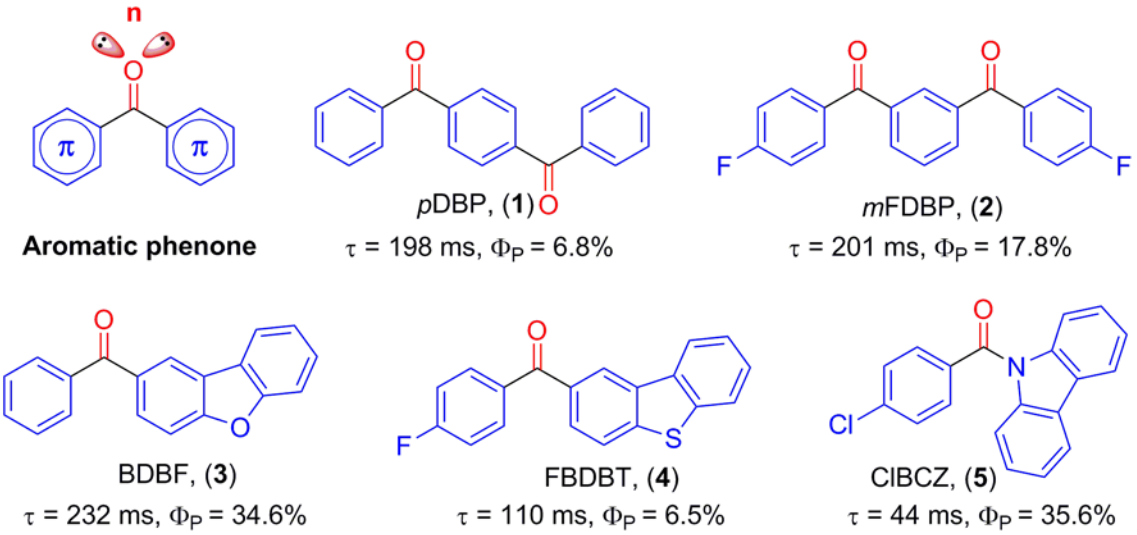


**Figure 3 | Structures of the organic molecules used in this research for tuning the RTP lifetimes and efficiencies.** The incorporation of carbonyl groups with non-bonding electrons aims to promote the effective intersystem crossing. The different aromatic substituents are introduced to support the formation of $^3(\pi, \pi^*)$ as lowest excited triplet state $T_1$ with variable energy level and mixing extent of n orbital.

So we extract the following rules for structural requirements of a purely organic persistent and efficient RTP phosphor without heavy atoms: existence of n orbital to trigger the effective SOC; $T_1$ with a nearly pure $^3(\pi,\pi^*)$ configuration to facilitate slow radiative decay pathway. Considering these rules, we design and synthesize five purely organic molecules containing carbonyl groups (C=O) and variable π–extended subunits (Figure 3). Note that the carbonyl groups are chose here from various hetero groups that can provide n orbitals to provide effective SOC-induced ISC. The promoted ISC process thus dominates the decay of $S_1$ state, leading to a high upper limit of $\Phi_P$ ($\Phi_{ISC}$). Another important element in these molecules is the essential π–extended subunits that make $T_1$ state has most character of $^3(\pi,\pi^*)$ configuration, leading to a persistent decay route. The molecular orbitals can be effectively mixed between pure $(n,\pi^*)$ and $(\pi,\pi^*)$ configurations through the variation of aryl groups, giving the whole

molecule tunable $T_1$ states in terms of energy level and $^3(\pi,\pi^*)$ character which are crucial for emission color, efficiency and lifetime of phosphorescence. Crystallization is chosen here to minimize quenching effect and other nonradiative decay pathways. As a result, remarkably fast $k_{ISC}$, tunable $k_P$ and slow $k_{nr}$ can be realized in our system.

**Theoretical Calculations**

To validity our assumption and gain more insights into the mechanism of RTP, we performed first-principle density functional theory (DFT) and time-dependent DFT (TD-DFT) investigations. For comparison, benzophenone (BP, **6**), benzil (**7**) and difluorobenzophenone (DFBP, **8**) are also included. The calculated energy gap, spin–orbit coupling constant ($\xi_{so}$) between the involved singlet and triplet state as well as the proportions of $^3$(n, $\pi^*$) configuration ($\alpha_n$) and $^3(\pi, \pi^*)$ configuration ($\beta_\pi$) is summarized in Figure sxx (Represented by BDBF in Figure 4a inset). The calculated energy gaps between $S_1$ and $T_1$ are considerably large for **1**-**8** (>0.6 eV), which block the reversible intersystem crossing process for TADF[29,30].

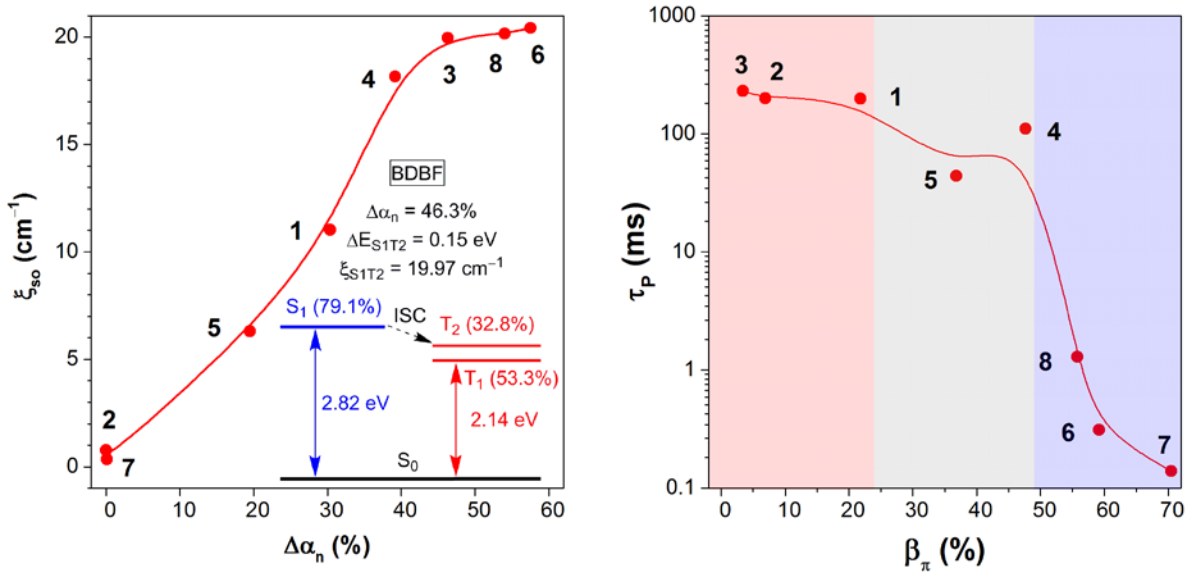


**Figure 4 | Theoretical calculations for mechanistic investigation. a**, Relationship between the calculated spin-orbital coupling constant ($\xi_{SO}$) and change of $^3$(n, $\pi^*$) configuration proportion ($\alpha_n$) during $S_1$ to $T_n$ transition through TD-DFT calculations. Inset: Diagrams showing the TD-DFT-calculated energy levels, main orbital configurations at singlet ($S_1$) and triplet ($T_n$) states, $\xi_{SO}$ of BDBF, note that data in parentheses give the $\alpha_n$ value. **b**, Plot of the calculated phosphorescence decay rate $k_P$ and experimental persistent lifetime $\tau_P$ against proportion of $^3(\pi, \pi^*)$ configuration ($\beta_\pi$) at $T_1$.

As shown in Figure 4a, the $\xi_{SO}$ is plotted against $\Delta\ \alpha_n$ during $S_1$ to $T_n$ transition. A considerable change of $\Delta\ \alpha_n$ always leads to the strong spin-orbital coupling. The reason should be that large $\Delta\ \alpha_n$ results high degree of n↔π transition, which provides essential single-center $p_x \rightarrow p_y$ transition. According to the El-Sayed's rule and the Franck–Condon principle, the ISC rate ($k_{ISC}$) is greatly promoted by small energy gap and large spin–orbit coupling. So the dominant channels for ISC will occur from the $S_1$ state to the $T_n$ state with a small energy splitting ($\Delta E_{ST}$) and a large $\Delta\ \alpha_n$.

Through analysis proportion of $^3$(n, $\pi^*$) configuration ($\alpha_n$) and $^3(\pi, \pi^*)$ configuration ($\beta_\pi$) in molecular orbitals, features of excited states are obtained. As shown in Figure 4b, when the $\beta_\pi$ is lower than 30%, a typical $^3$(n, $\pi^*$) orbital characteristic is shown as revealed in **6**, **7** and **8**; when the $\beta_\pi$ is increased to higher than 50% by aromatic subunits, a typical $^3(\pi, \pi^*)$ orbital characteristic is shown as revealed in **1**, **2**, and **3**. Generally, molecules with a $^3$(n, $\pi^*$)

configuration enjoys a faster $k_P$ than $^3(\pi, \pi^*)$ because of the spin-flip allowed process for the availability of n↔π and $p_x \rightarrow p_y$ transition.

Taking BDBF for example, it have a typical $^1$(n□□π□□□S$_1$ state and two excited triplet states ($T_1$ and $T_2$) lying below the $S_1$, suggesting the possible occurrence of ISCs of $S_1 \rightarrow T_1$ and $S_1 \rightarrow T_2$ transition channels. Relative small $\Delta E_{S1T2}$ energy gap and big value of $\Delta\ \alpha_n$ from $S_1$ to $T_2$ makes $S_1 \rightarrow T_2$ transition as the key channels to populating triplet states. The essential large value of $\beta_\pi$ in $T_1$ decides its $^3(\pi, \pi^*)$ feature, may lead to slow phosphorescent decay rate.

**Experimental Properties**

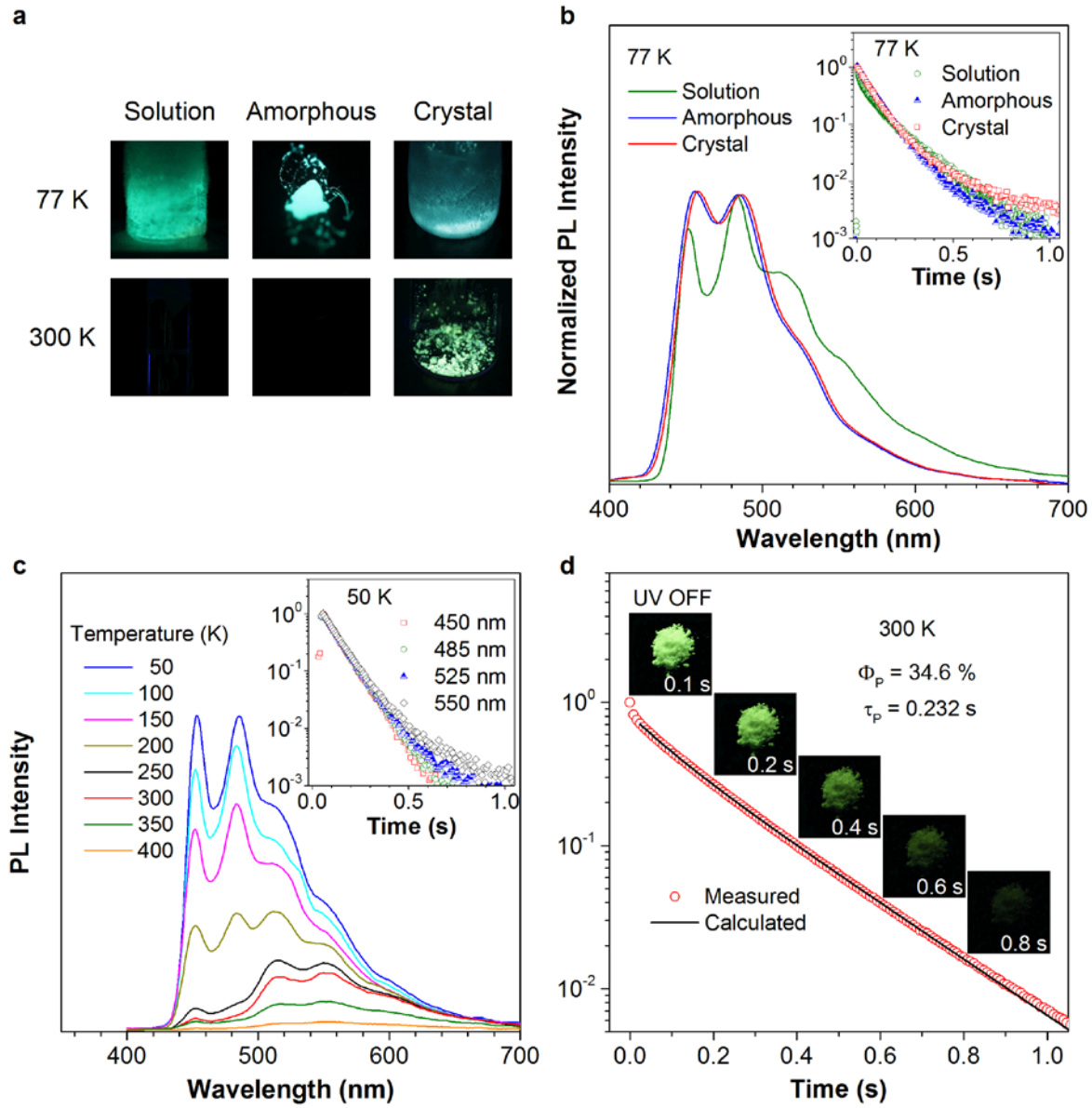


**Figure 5 | Photophyscial properties of BDBF. a**, Photographs of BDBF solution ($10^{-4}$ M in cyclohexane), amorphous powder, and crystalline powder under 365 UV irradiation at 77 K and 300 K, respectively. **b**, PL spectra of BDBF solution, amorphous powder, and crystalline powder at 77 K. Inset: Time-resolved PL decay curves of BDBF solution, amorphous powder, and crystalline powder at 525 nm measured at 77 K. **c**, PL spectra of BDBF measured at different temperatures from 50 to 400 K. Inset: Time-resolved PL decay curves of BDBF at 450, 485, 525 and 550 nm measured at 50 K indicating that the emission is pure phosphorescence. **d**, Time-resolved PL decay curve of BDBF at 300 K. Inset photographs show the time-dependent emission decay of BDBF crystals taken under 365 nm UV irradiation.

Benzophenone (**6**) is an archetypal phosphor, which exhibits short-lived (~ms) phosphorescence both in solution at low temperature[31] and in crystalline state at room temperature[16]. When substituted with different π–extended groups such as benzoyl, benzofuranyl, benzothiophenyl, and carbazolyl groups, five luminogens named as *p*DBP (**1**), *m*FDBP (**2**), BDBF (**3**), FBDBT (**4**), and ClBCZ (**5**) are afforded (Supplementary Information). Purified by recrystallization from dichloromethane solutions for twice, they are subjected for systematically photophysical properties investigation. They are found non-luminescent in solutions and amorphous states but strongly emissive at crystalline states at ambient conditions, indicating their crystallization-induced RTP (CI-RTP) characteristics belonged to aggregation-induced emission (AIE) system[32].

As a proof-of-concept, we take BDBF as the representative for illustrating the structure-property relationship. Upon ultraviolet (UV) irradiation at 365 nm, crystals of BDBF emit intensely at 77 K and 300 K in air. However, its solution and amorphous powder emit only at 77 K (Figure 5a). Together with almost identical steady-state photoluminescence (PL) spectra measured in air and in nitrogen atmosphere (Figure SXX), reveal that crystallization is an effective rigidification tool to trigger the RTP through blocking oxygen quenching and other nonradiative decay pathways. Very similar PL spectra and lifetime measurements of the BDBF molecules in different states are obtained at 77 K, revealing the intrinsic persistent phosphorescence features based on molecular structure (Figure 5b). In a further set of experiments, we investigate the temperature effect. On increasing the temperature from 50 to 350 K, the emission intensity of BDBF decrease, suggesting that the nonradiative decay of the excited states at elevated temperatures is likely to be enhanced (Figure 5c). Interestingly, time-resolved PL decay profiles measured at 50 K show that all the emission bands from 400 to 700 nm exhibit persistent lifetimes, proving the pure phosphorescent characteristic of luminescence. After removal of the excitation source, the emission slowly fades monitoring by naked eyes. Its luminescence lifetime is then measured to be 0.232 s, which is quite long among the reported RTP. It also maintains the intensive emission with a phosphorescence quantum yield of 34.6% at ambient conditions.

As mentioned above, π–extended aryl groups will largely influence the electronic properties of luminogens, resulting different emission behaviors. Tuning of emission color can be observed with the naked eye; compounds **1**–**5** exhibit bright photoluminescence in crystal, with emission color varying from blue to green, yellow to orange–red (Figure 6a Inset). This suggests that changing aromatic subunits effectively modulates the energy gap between $T_1$ and $S_0$. Steady-state PL spectra exhibited broad structureless shape suggesting the emission feature of $^3(\pi, \pi^*)$ rather than $^3(n, \pi^*)$. Lifetimes are then resulted in hundred milliseconds. In detail, *p*DBP (**1**) crystals emit yellow light with a quantum yield of 6.8%. *m*FBDBF (**2**) powders emit intense green light with an overall quantum yield of 17.8%. FBDBT (**4**) crystals emit pink light with a quantum yield of 6.5%. ClBCZ (**5**) crystals emit intensely green light with a highest quantum yield of 35.6% and a relative short lifetime of 44 ms. After removal of UV excitation, they are still high emissive without apparent change of appearance because of the quite similar prompted and delayed PL spectra, indicating their pure phosphorescence feature.

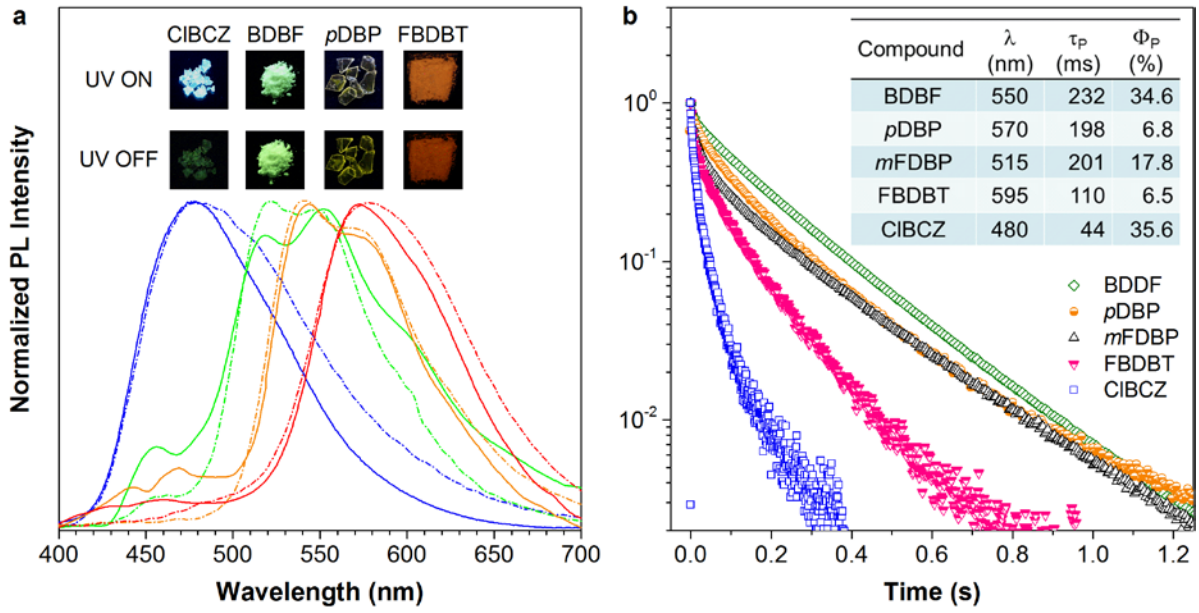


**Figure 6 | Versatile RTP molecules with tunable colors and lifetimes under ambient conditions**. **a**, The steady-state (solid) prompted and delayed phosphorescence (dash, 10 ms) spectra. Insets show the corresponding photographs taken before (up) and after (down) the excitation source is turned off. The compounds were excited at 365 nm at their crystalline states. **b**, Time-resolved PL decay curves of BDBF, *p*DBP, *m*FDBP, FBDBT and ClBCZ. Inset table summarizes their lifetimes and phosphorescence quantum yields.

## Discussion

Our experimental data reveals that tunable emission colors (from blue to red), high efficiencies (up to 35.6%), and persistent lifetimes (up to 0.23 s) are successfully achieved by using proper π system. Furthermore, persistent and efficient RTP is achieved upon one molecule BDBF under ambient conditions. Although the performance is impressive, both lifetime and efficiency is still poorer than the best one. Carefully examination the performance of reported systems reveals a conflict. Systems with high efficiency have short microseconds lifetimes[18,19] while that with persistent lifetime suffer low efficiency[20,24]. Equation (1) (Figure 2b) illustrates the relationship between $\Phi_P$ and $\tau_P$:

$$\Phi_P = \Phi_{ISC}(1-k_{nr}\tau_P)$$

Using the same rigidification methodology (crystallization here), the $k_{nr}$ is suppressed to almost the same level. Obviously the increase of lifetime will decrease the efficiency. On the other hand, persistent lifetime require smaller $k_P$ (i.e. $10^{-3}$ $s^{-1}$ in Huang's H-aggregation system[24]), resulting in a poorer ability of competition with $k_{nr}$. In contrast, short lifetime will increase the efficiency and enhance the competition ability of $k_P$ towards $k_{nr}$ (i.e. Kim's halogen bonding system[18,19]). Therefore, achieving high efficiency for persistent RTP system becomes much more difficult than that for short-lived RTP system[33]. Of course, if we can suppress the $k_{nr}$ to an ignorable level (~0 $s^{-1}$), we may still obtain both high efficiency and persistent RTP system. As a proof-of-concept, here we present the system with the balanced performance.

Revisit the Figure 4b which demonstrates correlation of measured $\tau_P$ and calculated $k_P$ against $\beta_\pi$. The coherence trend between $\tau_P$ and $1/k_P$ is easily understood and suggests that the $k_{nr}$ is suppressed to the same level. The positive correlation of $\tau_P$ against $\beta_\pi$ reveals that the molecular orbital feature of $T_1$ dominates the $k_P$. High $\beta_\pi$ decides nearly pure $^3(\pi, \pi^*)$ characteristic of $T_1$, which undergo persistent phosphorescence decay pathway as expected.

More importantly, the experimental results validate the molecular orbital model and theoretical calculations, which could serve as an attractive endeavor for searching the fundamental structure-property relationship.

## Conclusions

In conclusion, we presented a basic design principle for comprehensive understanding the phosphorescence lifetime and efficiency for purely organic materials. The principle, which involves adjusting the characteristic of molecular orbitals in excited states resulted from molecular structure, provides tool for modulating the RTP performance. Tunable lifetime, efficiency and color in a diverse array of purely organic phosphors were achieved by tailoring the structure of aromatic subunits. The key issue is synergistic effect of aromatic subunits and ketones, realizing remarkably fast $k_{ST}$ and slow $k_P$ to afford balanced performance. The rational guidelines gained from our experimental and theoretical investigations will allow for the exploration of novel organic phosphors.

## Methods

All the chemicals and other regents were purchased from Aldrich and used as received without further purification. All synthesized molecules were fully characterized by $^{1}$H-NMR, $^{13}$C-NMR, high resolution mass spectroscopy, element analysis and single-crystal X-ray analysis (see Supplementary Information). The IR spectra, steady-state ultraviolet−visible absorption spectra and photoluminescence spectra were measured on a Perkin-Elmer 16 PC FTIR spectrophotometer, a Milton Ray Spectronic 3000 Array spectrophotometer and a PerkinElmer LS 55 spectrophotometer, respectively. The lifetime, time-resolved excitation spectra, time-resolved emission spectra, temperature dependent photoluminescence spectra and absolute luminescent quantum yield were measured using an Edinburgh FLSP920 fluorescence spectrophotometer equipped with a xenon arc lamp (Xe900), a microsecond flash-lamp (uF900), a closed cycle cryostat(CS202*I-DMX-1SS, Advanced Research Systems) and a integrating sphere, respectively. Powder X-Ray diffraction (XRD) patterns were performed on an X'Pert PRO MPD diffractometer with Cu Kα radiation (λ = 1.5418 Å) at 25 °C (scan range: 4.5−50°). Single crystal data was collected on a Bruker Smart APEXII CCD diffractometer using graphite monochromated Cu Kα radiation (λ = 1.54178 Å). The photos and videos were recorded by a Cannon EOS 60D. The DFT and TD-DFT calculations were performed with the Gaussian 09 program.

## References


1 Pope, M., Kallmann, H. P. & Magnante, P. Electroluminescence in Organic Crystals. *J. Chem. Phys.* **38**, 2042-2043 (1963).

2 Maldiney, T. *et al.* Controlling Electron Trap Depth To Enhance Optical Properties of Persistent Luminescence Nanoparticles for In Vivo Imaging. *J. Am. Chem. Soc.* **133**, 11810-11815, doi:10.1021/ja204504w (2011).

3 Shao, Y. & Yang, Y. Efficient Organic Heterojunction Photovoltaic Cells Based on Triplet Materials. *Adv. Mater.* **17**, 2841-2844, doi:10.1002/adma.200501297 (2005).

4 Baldo, M. A. *et al.* Highly efficient phosphorescent emission from organic electroluminescent devices. *Nature* **395**, 151-154 (1998).

5 Hirata, S., Totani, K., Yamashita, T., Adachi, C. & Vacha, M. Large reverse saturable absorption under weak continuous incoherent light. *Nat. Mater.* **13**, 938-946, doi:10.1038/nmat4081
http://www.nature.com/nmat/journal/v13/n10/abs/nmat4081.html - supplementary-information (2014).

6 Sun, H. *et al.* Smart responsive phosphorescent materials for data recording and security protection. *Nat. Commun.* **5**, doi:10.1038/ncomms4601 (2014).

7 Zhang, G., Palmer, G. M., Dewhirst, M. W. & Fraser, C. L. A dual-emissive-materials design concept enables tumour hypoxia imaging. *Nat. Mater.* **8**, 747-751, doi:10.1038/nmat2509 (2009).

8 Menning, S. *et al.* Twisted tethered tolanes: unanticipated long-lived phosphorescence at 77 K. *J. Am. Chem. Soc.* **135**, 2160-2163, doi:10.1021/ja400416r (2013).
9 Zhang, Y., Lee, J. & Forrest, S. R. Tenfold increase in the lifetime of blue phosphorescent organic light-emitting diodes. *Nat. Commun.* **5**, doi:10.1038/ncomms6008 (2014).
10 Lee, J. *et al.* Deep blue phosphorescent organic light-emitting diodes with very high brightness and efficiency. *Nat. Mater.* **advance online publication**, doi:10.1038/nmat4446
http://www.nature.com/nmat/journal/vaop/ncurrent/abs/nmat4446.html - supplementary-information (2015).
11 Yoshii, R., Hirose, A., Tanaka, K. & Chujo, Y. Functionalization of boron diiminates with unique optical properties: multicolor tuning of crystallization-induced emission and introduction into the main chain of conjugated polymers. *J. Am. Chem. Soc.* **136**, 18131-18139, doi:10.1021/ja510985v (2014).
12 Zheng, X. *et al.* Hypoxia-specific ultrasensitive detection of tumours and cancer cells in vivo. *Nat. Commun.* **6**, doi:10.1038/ncomms6834 (2015).
13 Lee, D. *et al.* Room temperature phosphorescence of metal-free organic materials in amorphous polymer matrices. *J. Am. Chem. Soc.* **135**, 6325-6329, doi:10.1021/ja401769g (2013).
14 Kwon, M. S., Lee, D., Seo, S., Jung, J. & Kim, J. Tailoring intermolecular interactions for efficient room-temperature phosphorescence from purely organic materials in amorphous polymer matrices. *Angew. Chem. Int. Ed.* **53**, 11177-11181, doi:10.1002/anie.201404490 (2014).
15 Zhang, G. *et al.* Multi-emissive difluoroboron dibenzoylmethane polylactide exhibiting intense fluorescence and oxygen-sensitive room-temperature phosphorescence. *J. Am. Chem. Soc.* **129**, 8942-8943, doi:10.1021/ja0720255 (2007).
16 Yuan, W. Z. *et al.* Crystallization-Induced Phosphorescence of Pure Organic Luminogens at Room Temperature. *J. Phys. Chem. C* **114**, 6090-6099, doi:10.1021/jp909388y (2010).
17 Gong, Y. *et al.* Crystallization-induced dual emission from metal- and heavy atom-free aromatic acids and esters. *Chem. Sci.* **6**, 4438-4444, doi:10.1039/C5SC00253B (2015).
18 Bolton, O., Lee, K., Kim, H. J., Lin, K. Y. & Kim, J. Activating efficient phosphorescence from purely organic materials by crystal design. *Nature chemistry* **3**, 205-210, doi:10.1038/nchem.984 (2011).
19 Bolton, O., Lee, D., Jung, J. & Kim, J. Tuning the Photophysical Properties of Metal-Free Room Temperature Organic Phosphors via Compositional Variations in Bromobenzaldehyde/Dibromobenzene Mixed Crystals. *Chem. Mater.* **26**, 6644-6649, doi:10.1021/cm503678r (2014).
20 Hirata, S. *et al.* Efficient Persistent Room Temperature Phosphorescence in Organic Amorphous Materials under Ambient Conditions. *Adv. Funct. Mater.* **23**, 3386-3397, doi:10.1002/adfm.201203706 (2013).
21 Kwon, M. S. *et al.* Suppressing molecular motions for enhanced room-temperature phosphorescence of metal-free organic materials. *Nat Commun* **6**, doi:10.1038/ncomms9947 (2015).
22 Fermi, A., Bergamini, G., Roy, M., Gingras, M. & Ceroni, P. Turn-on phosphorescence by metal coordination to a multivalent terpyridine ligand: a new paradigm for luminescent sensors. *J. Am. Chem. Soc.* **136**, 6395-6400, doi:10.1021/ja501458s (2014).
23 Wang, H., Wang, H., Yang, X., Wang, Q. & Yang, Y. Ion-Unquenchable and Thermally "On–Off" Reversible Room Temperature Phosphorescence of 3-

Bromoquinoline Induced by Supramolecular Gels. *Langmuir : the ACS journal of surfaces and colloids* **31**, 486-491, doi:10.1021/la5040323 (2015).
24 An, Z. *et al.* Stabilizing triplet excited states for ultralong organic phosphorescence. *Nat. Mater.* **14**, 685-690, doi:10.1038/nmat4259 http://www.nature.com/nmat/journal/v14/n7/abs/nmat4259.html - supplementary-information (2015).
25 Gong, Y. *et al.* Achieving Persistent Room Temperature Phosphorescence and Remarkable Mechanochromism from Pure Organic Luminogens. *Adv. Mater.* **27**, 6195-6201, doi:10.1002/adma.201502442 (2015).
26 Mukherjee, S. & Thilagar, P. Recent advances in purely organic phosphorescent materials. *Chem. Commun.* **51**, 10988-11003, doi:10.1039/C5CC03114A (2015).
27 Lower, S. K. & El-Sayed, M. A. The Triplet State and Molecular Electronic Processes in Organic Molecules. *Chem. Rev.* **66**, 199-241, doi:10.1021/cr60240a004 (1966).
28 Turro, N. J., Scaiano, J. C. & Ramamurthy, V. (University Science Books, 2010).
29 Uoyama, H., Goushi, K., Shizu, K., Nomura, H. & Adachi, C. Highly efficient organic light-emitting diodes from delayed fluorescence. *Nature* **492**, 234-238, doi:http://www.nature.com/nature/journal/v492/n7428/abs/nature11687.html - supplementary-information (2012).
30 Goushi, K., Yoshida, K., Sato, K. & Adachi, C. Organic light-emitting diodes employing efficient reverse intersystem crossing for triplet-to-singlet state conversion. *Nat Photon* **6**, 253-258, doi:http://www.nature.com/nphoton/journal/v6/n4/abs/nphoton.2012.31.html - supplementary-information (2012).
31 Kearns, D. R. & Case, W. A. Investigation of Singlet → Triplet Transitions by the Phosphorescence Excitation Method. III. Aromatic Ketones and Aldehydes. *J. Am. Chem. Soc.* **88**, 5087-5097, doi:10.1021/ja00974a008 (1966).
32 Mei, J., Leung, N. L. C., Kwok, R. T. K., Lam, J. W. Y. & Tang, B. Z. Aggregation-Induced Emission: Together We Shine, United We Soar! *Chem. Rev.* **115**, 11718-11940, doi:10.1021/acs.chemrev.5b00263 (2015).
33 Xue, P. *et al.* Bright persistent luminescence from pure organic molecules through a moderate intermolecular heavy atom effect. *Chem. Sci.*, doi:10.1039/C5SC03739E (2016).

## Acknowledgements

The authors acknowledge the financial support by the National Basic Research Program of China, 973 Program (2013CB834701), the National Natural Science Foundation of China (21490570 and 21490574), the Research Grants Council of Hong Kong (604913, 6301614, 16305014, 16305015, and N_HKUST604/14), the University Grants Committee of Hong Kong (AoE/P-03/08), and the Innovation and Technology Commission (ITCPD/17-9). B.Z.T. thanks the financial support from the Guangdong Innovative Research Team Program (201101C0105067115).

## Author contributions

W.Z. synthesized all materials. W.Z. and Z.H. grew the crystals, made all photophysical measurements and analyses presented, and prepared the paper. So W.Z. and Z.H. contributed equally to this work. H.M. and Q.P. performed the theoretical calculations. G.B. and J.H. assisted the photophysical properties measurement. B.Z.T. designed and supervised the research and wrote the paper. All authors discussed the results and commented on the manuscript.

## Author information

Reprints and permissions information is available at www.nature.com/reprints. The authors declare no competing financial interests. Readers are welcome to comment on the online version of the paper. Correspondence and requests for materials should be addressed to B.Z.T. or Q.P. (tangbenz@ust.hk or qpeng@iccas.ac.cn).